

84. Leptonic Decays of Charged Pseudoscalar Mesons

Revised September 2019 by J.L. Rosner (Chicago U.), S.L. Stone (Syracuse U.) and R. Van de Water (FNAL).

84.1 Introduction

Charged mesons formed from a quark and antiquark can decay to a lepton-neutrino pair when these objects annihilate via a virtual W boson. Fig. 84.1 illustrates this process for the purely leptonic decay of a D^+ meson.

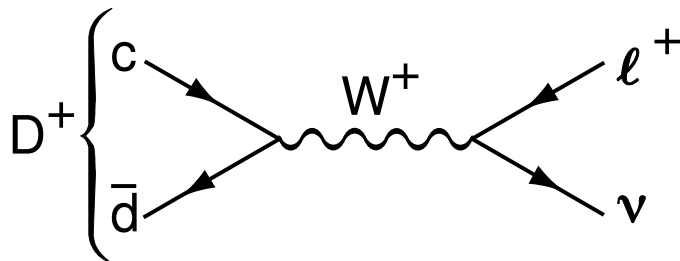


Figure 84.1: The annihilation process for pure D^+ leptonic decays in the standard model.

Similar quark-antiquark annihilations via a virtual W^+ to the $\ell^+\nu$ final states occur for the π^+ , K^+ , D_s^+ , and B^+ mesons. (Whenever pseudoscalar-meson charges are specified in this article, use of the charge-conjugate particles and corresponding decays are also implied.) Let P be any of these pseudoscalar mesons. To lowest order, the decay width is

$$\Gamma^{(0)}(P \rightarrow \ell\nu) = \frac{G_F^2}{8\pi} f_P^2 m_\ell^2 M_P \left(1 - \frac{m_\ell^2}{M_P^2}\right)^2 |V_{q_1 q_2}|^2. \quad (84.1)$$

Here M_P is the P mass, m_ℓ is the ℓ mass, $V_{q_1 q_2}$ is the Cabibbo-Kobayashi-Maskawa (CKM) matrix element between the quarks $q_1 \bar{q}_2$ in P , and G_F is the Fermi coupling constant. The decay constant f_P is proportional to the matrix element of the axial current between the one- P -meson state and the vacuum:

$$\langle 0 | \bar{q}_1 \gamma_\mu \gamma_5 q_2 | P(p) \rangle = i p_\mu f_P, \quad (84.2)$$

and can be thought of as the “wavefunction overlap” of the quark and antiquark. In this article we use the convention in which $f_\pi \approx 130$ MeV. For brevity, we will often denote the purely leptonic decay width in Eq. (84.1) by $\Gamma^{(0)}$.

The decay of P^\pm starts with a spin-0 meson, and ends up with a left-handed neutrino or right-handed antineutrino. By angular momentum conservation, the ℓ^\pm must then also be left-handed or right-handed, respectively. In the $m_\ell = 0$ limit, the decay is forbidden, and can only occur as a result of the finite ℓ mass. This helicity suppression is the origin of the m_ℓ^2 dependence of the decay width.

Experimentally, it is difficult to isolate events in which there are *only* a lepton and neutrino in the final state from those with a lepton, neutrino, and soft photon. Thus, radiative contributions must be removed from the experimental measurements *a posteriori* to obtain $\Gamma^{(0)}$. The radiative contributions can be broken into three pieces: the short-distance contribution to leptonic and semileptonic decays mediated by a W^\pm boson that accounts for electroweak corrections not included in the definition of G_F , the long-distance internal bremsstrahlung (IB) contribution, and the contribution from photon emission that depends upon the hadron’s structure. The universal

electroweak correction was calculated at $\mathcal{O}(\alpha)$ by Sirlin [1], and increases the purely leptonic decay rate by $\sim 1.8\text{--}2.2\%$ depending on the decaying meson. The $\mathcal{O}(\alpha)$ IB contribution was calculated by Kinoshita [2], and again is universal for all leptonic decays at this order. Numerically, the universal long-distance contribution lowers the purely leptonic decay rate by $\sim 0.4\text{--}2.4\%$, where the correction is smallest for pions and largest for $D_{(s)}$ mesons. The structure-dependent contributions have been estimated within various effective theories to increase the purely leptonic rate by one to a few percent [3–8].

In this review we treat the radiative corrections differently for the light, charm, and bottom meson systems for several reasons. First, the experimental uncertainties on the decay widths vary substantially. Thus, while the inclusion of radiative corrections is essential for the pion, kaon, and D -meson decay widths, which have been measured to (sub)-percent precision, radiative corrections can be neglected (for now) for $B \rightarrow \tau\nu$ decay. Second, the photons are treated differently on the experimental side for the different decay processes. For pions and kaons, the experimental measurements of $\Gamma_{P\ell 2[\gamma]}$ are fully inclusive, while for D mesons, the experiments impose cuts on the energy of any neutral cluster deposited in the calorimeter, which reduce the soft-photon background substantially. Some experiments also remove the QED bremsstrahlung in the leading-logarithmic approximation using the PHOTOS Monte-Carlo generator [9]. Third, the theoretical knowledge of the structure-dependent corrections varies for each meson system.

Once radiative corrections have been accounted for, measurements of purely leptonic decay branching fractions and lifetimes allow an experimental determination of the product $|V_{q_1 q_2}| f_P$. If the decay constant f_P is known to sufficient precision from theory, one can obtain the corresponding CKM element within the standard model. If, on the other hand, one takes the value of $|V_{q_1 q_2}|$ assuming CKM unitarity, one can infer an “experimental measurement” of the decay constant that can then be compared with theory.

The importance of measuring $\Gamma(P \rightarrow \ell\nu)$ depends on the particle being considered. Leptonic decays of charged pseudoscalar mesons occur at tree level within the standard model. Thus one does not expect large new-physics contributions to measurements of $\Gamma(P \rightarrow \ell\nu)$ for the lighter mesons $P = \pi^+, K^+$, and these processes in principle provide clean standard-model determinations of $|V_{ud}|$ and $|V_{us}|$. The situation is different for leptonic decays of charm and bottom mesons. The presence of new heavy particles such as charged Higgs bosons or leptoquarks could lead to observable effects in $\Gamma(P \rightarrow \ell\nu)$ for $P = D_{(s)}^+, B^+$ [10–14]. Thus the determination of $|V_{ub}|$ from $B^+ \rightarrow \tau\nu$ decay, in particular, should be considered a probe of new physics. More generally, the ratio of leptonic decays to $\tau\nu$ over $\mu\nu$ final states probes lepton universality [10, 15].

The determinations of CKM elements from leptonic decays of charged pseudoscalar mesons provide complementary information to those from other decay processes. The decay $P \rightarrow \ell\nu$ proceeds in the standard model via the axial-vector current $\bar{q}_1 \gamma_\mu \gamma_5 q_2$, whereas semileptonic pseudoscalar meson decays $P_1 \rightarrow P_2 \ell\nu$ proceed via the vector current $\bar{q}_1 \gamma_\mu q_2$. Thus the comparison of determinations of $|V_{q_1 q_2}|$ from leptonic and semileptonic decays tests the $V - A$ structure of the standard-model electroweak charged-current interaction. More generally, a small right-handed admixture to the standard-model weak current would lead to discrepancies between $|V_{q_1 q_2}|$ obtained from leptonic pseudoscalar-meson decays, exclusive semileptonic pseudoscalar-meson decays, exclusive semileptonic baryon decays, and inclusive semileptonic decays [16, 17].

Both measurements of the decay rates $\Gamma(P \rightarrow \ell\nu)$ and theoretical calculations of the decay constants f_P for $P = \pi^+, K^+, D_{(s)}^+$ from numerical lattice-QCD simulations are now quite precise. As a result, the elements of the first row of the CKM matrix $|V_{ud}|$ and $|V_{us}|$ can be obtained to sub-percent precision from $\pi^+ \rightarrow \ell\nu$ and $K^+ \rightarrow \ell\nu$, where the limiting error is from theory. The elements of the second row of the CKM matrix $|V_{cd(s)}|$ can be obtained from leptonic decays

of charged pseudoscalar mesons to few-percent precision, where here the limiting error is from experiment. These enable stringent tests of the unitarity of the first and second rows of the CKM matrix.

This review is organized as follows. Because the experimental and theoretical issues associated with measurements of pions and kaons, charmed mesons, and bottom mesons differ, we discuss each one separately. We begin with the pion and kaon system in Sec. 84.2. First, in Sec. 84.2.1 we review current measurements of the experimental decay rates. We provide tables of branching-ratio measurements and determinations of the product $|V_{ud(s)}|f_{\pi+(K+)}$, as well as average values for these quantities including correlations and other effects needed to combine results. Then, in Sec. 84.2.2 we summarize the status of theoretical calculations of the decay constants. We provide tables of recent lattice-QCD results for $f_{\pi+}$, f_{K+} , and their ratio from simulations including dynamical u, d, s , and (in some cases c) quarks, along with averages including correlations and strong SU(2)-isospin breaking corrections as needed. We next discuss the charmed meson system in Sec. 84.3, again reviewing current experimental rate measurements in Sec. 84.3.1 and theoretical decay-constant calculations in Sec. 84.3.2. Last, we discuss the bottom meson system in Sec. 84.4, following the same organization as the two previous sections. For almost all of the decay constants presented in Secs. 84.2.2, 84.3.2, and 84.4.2, we take as our preferred values the four-flavor averages from 2019 Flavor Lattice Averaging Group (FLAG) review [18], which incorporate all lattice-QCD results that appeared before 30 September 2018. There have not been any new decay-constant results that would qualify for the FLAG average since then.

After having established the status of both experimental measurements and theoretical calculations of leptonic charged pseudoscalar-meson decays, we discuss some implications for phenomenology in Sec. 84.5. For each process discussed in Secs. 84.2–84.4, we combine the average $\mathcal{B}(P \rightarrow \ell\nu)$ with the decay constant f_P to infer the associated CKM matrix element. We then compare these results with determinations of the same CKM elements from other processes. We also use the CKM elements obtained from leptonic decays to test the unitarity of the first and second rows of the CKM matrix. Further, as in previous reviews, we combine the experimental $\mathcal{B}(P \rightarrow \ell\nu)$ s with the associated CKM elements obtained from CKM unitarity to infer “experimental” values for the decay constants. The comparison of these values with theory provides a test of lattice and other QCD approaches, assuming that new-physics contributions to these processes are not significant.

84.2 Pions and kaons

84.2.1 *Experimental rate measurements*

Experimental rate measurements of pion and kaon leptonic decays are fully radiation inclusive. Following Refs. [19, 20], and references therein, we combine the $\mathcal{O}(\alpha)$ radiative corrections to the purely leptonic rate as follows:

$$\Gamma(P \rightarrow \ell\nu[\gamma]) = \Gamma(P \rightarrow \ell\nu) \left[1 + \frac{\alpha}{\pi} C_P \right], \quad (84.3)$$

where $P = \pi, K$. The full expressions for C_π and C_K are given in Eq. (114) of Ref. [5]. In addition to the universal short- [1] and long-distance [2] corrections, C_π and C_K include hadronic-structure dependent contributions [3] through $\mathcal{O}(\alpha p^4)$ in chiral perturbation theory (χ PT), where p is the pion or kaon momentum. The inclusion of radiative corrections to the purely leptonic rates is numerically important given the level of precision achieved on the experimental measurements of the $\pi^\pm \rightarrow \mu^\pm\nu$ and $K^\pm \rightarrow \mu^\pm\nu$ decay widths.

We evaluate $\delta_P \equiv (\alpha/\pi)C_P$ using the latest experimentally-measured meson and lepton masses and coupling constants from the Particle Data group [21], and taking the low-energy constants

(LECs) that parameterize the hadronic contributions from Refs. [5, 22, 23]. Because the finite non-logarithmic parts of the LECs were estimated within the large- N_C approximation assuming that contributions from the lowest-lying resonances dominate, we conservatively assign a 100% uncertainty to the LECs, which leads to a ± 0.9 error in $C_{\pi,K}$.¹ We obtain the following correction factors to the individual charged pion and kaon decay widths:

$$\delta_\pi = 0.0176(21) \quad \text{and} \quad \delta_K = 0.0107(21). \quad (84.4)$$

The error on the ratio of kaon-to-pion leptonic decay widths is under better theoretical control because the hadronic contributions from low-energy constants estimated within the large- N_c framework cancel at lowest order in the chiral expansion. For the ratio, we use the correction factor

$$\delta_{K/\pi} = -0.0069(17), \quad (84.5)$$

where we take the estimated error due to higher-order corrections in the chiral expansion from Ref. [25].

There have been no new measurements of the pion leptonic decay rate since our previous review [26]. The sum of branching fractions for $\pi^- \rightarrow \mu^- \bar{\nu}$ and $\pi^- \rightarrow \mu^- \bar{\nu} \gamma$ is 99.98770(4)% [21]. Together with the lifetime 26.033(5) ns [21] this implies $\Gamma(\pi^- \rightarrow \mu^- \bar{\nu}[\gamma]) = 3.8408(7) \times 10^7 \text{ s}^{-1}$. We then subtract the estimated radiative correction factor δ_π in Eq. (84.4) to obtain the purely leptonic rate $\Gamma^{(0)}(\pi^- \rightarrow \mu^- \bar{\nu})$. Using this rate and the masses from the 2014 PDG review [21] in Eq. (84.1) gives

$$f_{\pi^-} |V_{ud}| = (127.13 \pm 0.02 \pm 0.13) \text{ MeV}, \quad (84.6)$$

where the errors are from the experimental rate measurement and the radiative correction factor, respectively.

The uncertainty on $f_{\pi^-} |V_{ud}|$ is dominated by that from theoretical estimate of the hadronic structure-dependent radiative corrections. Recently the first direct lattice-QCD calculation of the radiative corrections to the pion and kaon leptonic decay rates was performed by the RM123-Soton Collaboration [8]. The results for both $\delta_\pi = 0.0153(19)$ and $\delta_K = 0.0088(9)$, which are given in the Gasser-Rusetsky-Scimemi scheme [27], are compatible with our chiral-perturbation-theory estimates above and have smaller quoted uncertainties, especially for δ_K . While independent confirmation of these results is needed, they demonstrate a promising approach for reducing the theoretical uncertainties on the pion and kaon leptonic decay rates in the future.

The world average for the $K \rightarrow \mu\nu$ decay rate is obtained from a global fit of several kaon-decay branching ratios and lifetime measurements, and was last updated by the FlaviaNet Working Group on Kaon Decays in 2014 [28]. Thus, the radiation-inclusive branching ratio $\mathcal{B}(K^- \rightarrow \mu^- \bar{\nu}[\gamma]) = 63.58(11)\%$ and lifetime $\tau_{K^\pm} = 12.384(15) \text{ ns}$ are unchanged from our previous review. These measurements imply $\Gamma(K^- \rightarrow \mu^- \bar{\nu}[\gamma]) = 5.134(11) \times 10^7 \text{ s}^{-1}$. As before, we subtract δ_K in Eq. (84.4) from the radiation-inclusive decay width to obtain $\Gamma^{(0)}(K^- \rightarrow \mu^- \bar{\nu})$. We then use Eq. (84.1) to obtain

$$f_{K^+} |V_{us}| = (35.09 \pm 0.04 \pm 0.04) \text{ MeV}, \quad (84.7)$$

where the errors are from the experimental rate measurement and the radiative correction factor, respectively.

¹This uncertainty on $C_{\pi,K}$ is smaller than the error estimated by Marciano and Sirlin in Ref. [24], which predates the calculations of the hadronic-structure contributions in Refs. [3, 5, 22, 23]. The hadronic LECs incorporate the large short-distance electroweak logarithm discussed in Ref. [24], and their dependence on the chiral renormalization scale cancels the scale-dependence induced by chiral loops, thereby removing the dominant scale uncertainty of the Marciano–Sirlin analysis [24].

Short-distance radiative corrections cancel in the ratio of pion-to-kaon decay rates [29]:

$$\frac{\Gamma_{K\ell 2[\gamma]}}{\Gamma_{\pi\ell 2[\gamma]}} = \frac{|V_{us}|^2 f_{K^-}^2}{|V_{ud}|^2 f_{\pi^-}^2} \frac{m_K(1 - m_\ell^2/m_K^2)^2}{m_\pi(1 - m_\ell^2/m_\pi^2)^2} (1 + \delta_{K/\pi}), \quad (84.8)$$

where $\delta_{K/\pi}$ is given in Eq. (84.5). The left-hand side of Eq. (84.8) is 1.3367(28), which implies

$$\frac{|V_{us}|f_{K^-}}{|V_{ud}|f_{\pi^-}} = 0.27599 \pm 0.00029 \pm 0.00024, \quad (84.9)$$

where the first uncertainty is from the branching fractions and the second is from $\delta_{K/\pi}$. Here, the estimated error on the hadronic structure-dependent radiative corrections is commensurate with the experimental error.

In summary, the main experimental results pertaining to charged pion and kaon leptonic decays are

$$|V_{ud}|f_{\pi^-} = (127.13 \pm 0.02 \pm 0.13) \text{ MeV}, \quad (84.10)$$

$$|V_{us}|f_{K^+} = (35.09 \pm 0.04 \pm 0.04) \text{ MeV}, \quad (84.11)$$

$$\frac{|V_{us}|f_{K^+}}{|V_{ud}|f_{\pi^-}} = 0.27599 \pm 0.00029 \pm 0.00024, \quad (84.12)$$

where the errors are from the experimental uncertainties in the branching fractions and the theoretical uncertainties in the radiative correction factors δ_P , respectively. All of these values are the same as in our previous review [26].

84.2.2 *Theoretical decay-constant calculations*

Table 84.1 presents recent published results for the charged pion and kaon decay constants and their ratio from numerical lattice-QCD simulations with three ($N_f = 2 + 1$) or four flavors ($N_f = 2 + 1 + 1$) of dynamical quarks. The uncertainties on both the individual decay constants and their ratio are at the sub-percent level. The SU(3)-breaking ratio f_{K^+}/f_{π^+} can be obtained with especially small errors because statistical errors associated with the Monte Carlo simulations are correlated between the numerator and denominator, as are some systematics. The results in Table 84.1 were obtained using several independent sets of gauge-field configurations, and a variety of lattice fermion actions that are sensitive to different systematic uncertainties.² Thus, the good agreement between them indicates that the lattice-QCD uncertainties are controlled and the associated error estimates are reliable.³

Table 84.1 also shows the three- and four-flavor averages for the pion and kaon decay constants and their ratio from the 2019 Flavour Lattice Averaging Group (FLAG) review [18] in the lines labeled ‘‘FLAG 19 average.’’ There is no four-flavor average for the pion decay constant in Table 84.1 because all of the four-flavor calculations use the quantity f_{π^+} as an input to fix the absolute lattice scale needed to convert from lattice-spacing units to GeV [7, 35, 36].

All of the results in Table 84.1 were obtained using isospin-symmetric gauge-field configurations, *i.e.*, the dynamical up and down quarks have the same mass. Fortunately, however, the dominant effect of strong-isospin breaking is easily included in lattice-QCD calculations as follows. Because the up-down mass difference $\Delta m_{ud} \equiv (m_u - m_d) \sim -2.5 \text{ MeV}$ [18, 43] is much less than typical

²See the PDG mini-review on ‘‘Lattice Quantum Chromodynamics’’ [30] for a general review of numerical lattice-QCD simulations. Details on the different methods used in modern lattice-QCD calculations are provided in Appendix A of the FLAG ‘‘Review[s] of lattice results concerning low energy particle physics’’ [18, 31, 32].

³See the review by Kronfeld [33] for a summary of the large body of evidence validating the methods employed in modern lattice-QCD simulations.

Table 84.1: Recent published lattice-QCD results for f_{π^+} , f_{K^+} , and their ratio. The upper and lower panels show $(2 + 1 + 1)$ -flavor and $(2 + 1)$ -flavor determinations, respectively. When two errors are shown, they are statistical and systematic, respectively. Results for f_{π} and f_K in the isospin-symmetric limit $m_u = m_d$ are noted with an “*”; they are corrected for isospin breaking via Eq. (84.13) before computing the averages.

Reference	N_f	f_{π^+} (MeV)	f_{K^+} (MeV)	f_{K^+}/f_{π^+}
Fermilab/MILC 17 [34] [†]	2+1+1	–	–	1.1950(15) $^{(+6)}_{(-18)}$
ETM 14 [35] [†]	2+1+1	–	154.4(1.5)(1.3)	1.184(12)(11)
Fermilab/MILC 14 [7] [†]	2+1+1	–	155.92(13) $^{(+42)}_{(-34)}$	1.1956(10) $^{(+26)}_{(-18)}$ [‡]
HPQCD 13 [36] [†]	2+1+1	–	155.37(20)(28)	1.1916(15)(16)
FLAG 19 average [18]	2+1+1	–	155.7(3)	1.1932(19)
QCDSF/UKQCD 16 [37]	2+1	–	–	1.190(10)(13)
BMW 16 [38]	2+1	–	–	1.178(10)(26)
RBC/UKQCD 14 [39]*	2+1	130.19(89)	155.51(83)	1.1945(45)
MILC 10 [40]	2+1	129.2(0.4)(1.4)	156.1(4) $^{(+6)}_{(-9)}$	1.197(2) $^{(+7)}_{(-3)}$
BMW 10 [41]*	2+1	–	–	1.192(7)(6)
HPQCD/UKQCD 07 [42]*	2+1	132(2)	157(2)	1.189(2)(7)
FLAG 19 average [18]	2+1	130.2(8)	155.7(7)	1.1917(37)

[†] PDG 2014 value of $f_{\pi^+} = 130.41(21)$ MeV used to set absolute lattice scale.

[‡] Superseded by f_{K^+}/f_{π^+} from Fermilab/MILC 17.

hadronic scales, the strong-isospin breaking corrections to physical observables can systematically be expanded in the small parameter $\delta m_{ud} \equiv \Delta m_{ud}/\Lambda_{\text{QCD}}$. The leading strong-isospin-breaking corrections to pseudoscalar-meson decay constants arise from the light *valence* quarks in the initial- and final-state hadrons. (See, *e.g.*, the discussion in Ref. [44], for a detailed discussion of isospin-breaking effects in pion and kaon observables.) Thus, to include the effect of nondegenerate up- and down-quark masses, most recent lattice-QCD calculations of f_{π^+} and f_{K^+} evaluate the masses of the valence quarks in the pion at the physical m_u and m_d , and the mass of the valence light quark in the kaon at the physical m_u . This procedure yields a correction to the kaon decay constant below 0.5%. Consequently, strong-isospin breaking corrections from the light sea-quark masses – which are suppressed by an additional power of δm_{ud} – can be neglected given present uncertainties.

Some earlier lattice-QCD calculations, however, only provide the decay constants and their ratio in the $SU(2)$ isospin-symmetric limit [39, 41, 42]. The Flavour Lattice Averaging Group corrects these results for strong-isospin breaking using chiral perturbation theory before including them in the averages. The leading strong-isospin-breaking corrections to the pion and kaon decay constants in χPT can be parameterized as [25, 45]

$$f_{\pi^+} = f_{\pi}, \quad f_{K^+} = f_K \sqrt{1 + \delta_{SU(2)}}, \quad (84.13)$$

where f_{π} and f_K denote the values of the decay constants in the isospin-symmetric limit. The pion decay constant does not receive corrections linear in $m_u - m_d$ because of the G -parity symmetry of the pion triplet, so at first order the δm_{ud} expansion, strong-isospin breaking corrections are characterized by a single parameter, $\delta_{SU(2)}$. Next-to-leading order χPT yields numerical values for $\delta_{SU(2)}$ of approximately -0.004 . Recent direct lattice-QCD calculations of $\delta_{SU(2)}$ give larger values of around -0.005 to -0.008 [8, 34–36, 44, 46], but further studies are needed. Thus, to be conservative, FLAG includes an uncertainty of 100% on the χPT estimate for $\delta_{SU(2)}$ when correcting those decay-constant values that are quoted in the isospin-symmetric limit.

The errors on the decay-constant results in Table 84.1 obtained from $(2+1)$ -flavor lattice-QCD simulations do not include an estimate of the systematic uncertainty from the omission of charm sea quarks in the simulation. Consequently, when the uncertainty on the $(2+1+1)$ -flavor FLAG average is comparable to or better than that on the $(2+1)$ -flavor FLAG average, we simply use the four-flavor average as our preferred value. This is not possible, however, for the pion decay constant. To account for this, we first estimate the systematic uncertainty on pseudoscalar-meson decay constants associated with the omission of charm sea quarks. We then add this estimate in quadrature to the quoted error on the $(2+1)$ -flavor FLAG average for f_{π^+} to obtain our preferred value.

The error introduced by omitting charm sea quarks can be roughly estimated by expanding the charm-quark determinant in powers of $1/m_c$ [47]; the resulting leading contribution is of order $\alpha_s (\Lambda_{\text{QCD}}/2m_c)^2$ [48]. Taking the $\overline{\text{MS}}$ values $\overline{m}_c(\overline{m}_c) = 1.275$ GeV, $\overline{\Lambda}_{\text{QCD}} \sim 340$ MeV from FLAG [31], and $\overline{\alpha}(\overline{m}_c) \sim 0.4$, leads to an estimate of about 0.7% for the contribution to the decay constants from charm sea quarks. We can compare this power-counting estimate of charm sea-quark contributions with the observed differences between the $(2+1)$ - and $(2+1+1)$ -flavor lattice-QCD averages for kaon, $D_{(s)}$ -meson, and $B_{(s)}$ -decay constants in Tables 84.1, 84.4, and 84.6. Looking at Table 84.1, the three- and four-flavor averages for f_{K^+} agree to much better than our simple power-counting estimate. Inspection of Tables 84.4 and 84.6 shows, however, that charm sea-quark effects of this size are still allowed for both $D_{(s)}$ -meson and $B_{(s)}$ -meson decay constants.

Our final preferred theoretical values for the charged pion and kaon decay constants are

$$f_{\pi^+} = 130.2(1.2) \text{ MeV}, \quad f_{K^+} = 155.7(3) \text{ MeV}, \quad \frac{f_{K^+}}{f_{\pi^+}} = 1.193(2), \quad (84.14)$$

where f_{K^+} and f_{K^+}/f_{π^+} are simply the four-flavor FLAG 2019 averages [18], and f_{π^+} is the three-flavor flavor FLAG 2019 average with the error increased by the estimated 0.7% charm sea-quark contribution. The errors on all three quantities in Eq. (84.14) have decreased since our previous review [26, 49].

84.3 Charmed mesons

84.3.1 *Experimental rate measurements*

Measurements have been made of the branching fractions for D^+ and D_s^+ mesons decaying to both $\mu^+\nu$ and $\tau^+\nu$ final states. The CLEO-c, BES, and BES III experiments have made measurements of D^+ decays using e^+e^- collisions at the $\psi(3770)$ resonant energy where D^-D^+ pairs are copiously produced. They fully reconstruct one of the D 's; for concreteness, we will take this to be the D^- . Counting the number of these events provides the normalization for the branching fraction measurement. The experimental analyses then proceed by identifying a candidate μ^+ and forming the missing-mass squared, $MM^2 = (E_{\text{CM}} - E_{D^-})^2 - (\vec{p}_{\text{CM}} - \vec{p}_{D^-} - \vec{p}_{\mu^+})^2$, where E_{CM} and p_{CM} are the center-of-mass energy (which is known) and momentum (which equals zero in e^+e^- collisions). A peak at zero MM^2 implies the existence of a missing neutrino, and hence the $\mu^+\nu$ decay of the D^+ . CLEO-c does not explicitly identify the muon, so their data consists of a combination of $\mu^+\nu$ and $\tau^+\nu$, $\tau^+ \rightarrow \pi^+\nu$ events. This permits them to do two fits: in one they fit for the individual components, and in the other they fix the ratio of $\tau^+\nu/\mu^+\nu$ events to be that given by the standard-model expectation. Thus, the former measurement should be used for new-physics searches, and the latter for standard-model predictions. Our average uses the fixed-ratio value.

Table 84.2 shows the available measurements of $D^+ \rightarrow \mu^+\nu$, as an upper limit on $D^+ \rightarrow \tau^+\nu$ from CLEO-c and the first measurement of this decay from BES III. To extract the values of $|V_{cd}|f_{D^+}$ via Eq. (84.1), we use values of $m_{D^+} = 1.86961$ GeV and the well-measured D^+ lifetime

of 1.040(7) ps [50], and apply radiative corrections as described below. For calculating the average $\mu^+\nu$ number, we use the CLEO-c result from $\mu^+\nu^+ + \tau^+\nu$.

Table 84.2: Experimental results for $\mathcal{B}(D^+ \rightarrow \mu^+\nu[\gamma])$, $\mathcal{B}(D^+ \rightarrow \tau^+\nu[\gamma])$, and $|V_{cd}|f_{D^+}$. The systematic errors on the inferred values of $|V_{cd}|f_{D^+}$ include those from the D^+ lifetime and mass. The error from radiative corrections is only included in the entries labeled “our average.”

Experiment	Mode	\mathcal{B}	$ V_{cd} f_{D^+}$ (MeV)
CLEO-c [51, 52]	$\mu^+\nu$	$(3.93 \pm 0.35 \pm 0.09) \times 10^{-4}$	$46.70 \pm 2.10 \pm 0.55$
CLEO-c [51, 52]	$\mu^+\nu + \tau^+\nu$	$(3.82 \pm 0.32 \pm 0.09) \times 10^{-4}$	$46.00 \pm 1.91 \pm 0.56$
BES III [53]	$\mu^+\nu$	$(3.71 \pm 0.19 \pm 0.06) \times 10^{-4}$	$45.33 \pm 1.17 \pm 0.38$
Our average	Lines 2+3	$(3.74 \pm 0.17) \times 10^{-4}$	45.50 ± 1.22
CLEO-c [54, 55]	$\tau^+\nu$ ($\pi^+\bar{\nu}$)	$< 1.2 \times 10^{-3}$	
BES III [56]	$\tau^+\nu$ ($\pi^+\bar{\nu}$)	$(1.20 \pm 0.24 \pm 0.12) \times 10^{-3}$	49.95 ± 2.48
Our average	$\mu^+\nu + \tau^+\nu$		46.17 ± 1.16

To obtain the purely leptonic rates $\Gamma^{(0)}(D^+ \rightarrow \mu^+(\tau^+)\nu)$, we subtract the radiative contributions as in Sec. 84.2.1, but use numerical values for the corrections appropriate for D mesons. First, we reduce both the $\mu^+\nu$ and $\tau^+\nu$ branching fractions in Table 84.2 by 1.8%, which is the universal short-distance electroweak contribution of Sirlin [1] evaluated using the D -meson mass for the factorization scale. We do not adjust the experimental rates by the universal long-distance correction [2]. This is because QED bremsstrahlung contributions have already been subtracted at leading-log order from the measurements in Table 84.2 using Monte-Carlo estimates computed with PHOTOS [9]. The $\mu^+\nu$ rates should also be reduced by the 1% estimate of the structure-dependent contributions from Dobrescu and Kronfeld [14]. This correction accounts for tree-level radiative processes in which the D meson decays into a real photon and an off-shell vector meson, which subsequently decays weakly to a charged lepton and neutrino. It is estimated using Eq. (12) of Burdman *et al.* [4] with the CLEO-c cut on the photon energy from Ref. [65], which is typical of all the measurements. We do not need to apply the structure-dependent correction to the $\mu^+\nu$ branching fractions in Table 84.2, however, because the experiments have already included it in their quoted results. Therefore, in summary, we reduce both the $D^+ \rightarrow \mu^+\nu$ and the $D^+ \rightarrow \tau^+\nu$ rates by 1.8% to account for radiative corrections. It is worth noting, however, that the universal long-distance electromagnetic contribution estimated for point-like charged mesons by Kinoshita [2], which we are not including because IB contributions are already subtracted from the measurements via PHOTOS, would *increase* both rates by about 2.5%.

We now discuss the D_s^+ decay process. Measurements of the leptonic decay rate have been made by several groups and are listed in Table 84.3. We exclude older values obtained by normalizing to D_s^+ decay modes that are not well defined. Many measurements, for example, used the $\phi\pi^+$ mode. This decay is a subset of the $D_s^+ \rightarrow K^+K^-\pi^+$ channel which has interferences from other modes populating the K^+K^- mass region near the ϕ , the most prominent of which is the $f_0(980)$. Thus, the extraction of the effective $\phi\pi^+$ rate is sensitive to the mass resolution of the experiment and the cuts used to define the ϕ mass region [66].⁵

To find D_s decays in the $\mu^+\nu$ signal channels, the experiments rely on fully reconstructing all of the final state particles except for the neutrino and using a missing-mass technique to infer the existence of the neutrino. CLEO and BES III use $e^+e^- \rightarrow D_s D_s^*$ collisions at 4170 MeV, while

⁵We have not included the BaBar result for $\mathcal{B}(D_s^+ \rightarrow \mu^+\nu)$ reported in Ref. [67] because this measurement determined the ratio of the leptonic decay rate to the hadronic decay rate $\Gamma(D_s^+ \rightarrow \ell^+\nu)/\Gamma(D_s^+ \rightarrow \phi\pi^+)$.

Table 84.3: Experimental results for $\mathcal{B}(D_s^+ \rightarrow \mu^+\nu[\gamma])$, $\mathcal{B}(D_s^+ \rightarrow \tau^+\nu[\gamma])$, and $|V_{cs}|f_{D_s^+}$. The systematic errors on the inferred values of $|V_{cs}|f_{D_s^+}$ include those from the D^+ lifetime and mass. The entries labeled “our average” take into account correlations between systematic errors common to the experiments, and also include errors from radiative corrections.

Experiment	Mode	$\mathcal{B}(\%)$	$ V_{cs} f_{D_s^+}$ (MeV)
CLEO-c [54, 55]	$\mu^+\nu$	$(0.565 \pm 0.045 \pm 0.017)$	$247.6 \pm 9.9 \pm 4.1$
BaBar ⁴ [58]	$\mu^+\nu$	$(0.602 \pm 0.038 \pm 0.034)$	$254.3 \pm 8.0 \pm 7.4$
Belle [59]	$\mu^+\nu$	$(0.531 \pm 0.028 \pm 0.020)$	$238.8 \pm 6.3 \pm 4.8$
BES III [60]	$\mu^+\nu$	$(0.549 \pm 0.016 \pm 0.015)$	$244.9 \pm 3.6 \pm 3.7$
Our average	$\mu^+\nu$	(0.552 ± 0.016)	244.0 ± 5.2
CLEO-c [54, 55]	$\tau^+\nu$ ($\pi^+\bar{\nu}$)	$(6.42 \pm 0.81 \pm 0.18)$	$267.3 \pm 16.9 \pm 4.2$
CLEO-c [61]	$\tau^+\nu$ ($\rho^+\bar{\nu}$)	$(5.52 \pm 0.57 \pm 0.21)$	$247.9 \pm 12.8 \pm 5.0$
CLEO-c [62, 63]	$\tau^+\nu$ ($e^+\nu\bar{\nu}$)	$(5.30 \pm 0.47 \pm 0.22)$	$242.9 \pm 10.8 \pm 5.3$
BaBar [58]	$\tau^+\nu$ ($e^+(\mu^+)\nu\bar{\nu}$)	$(5.00 \pm 0.35 \pm 0.49)$	$236.9 \pm 8.3 \pm 11.7$
Belle [59]	$\tau^+\nu$ ($\pi^+\bar{\nu}$)	$(6.04 \pm 0.43^{+0.46}_{-0.40})$	$260.3 \pm 9.3^{+10.1}_{-8.8}$
Belle [59]	$\tau^+\nu$ ($e^+\nu\bar{\nu}$)	$(5.37 \pm 0.33^{+0.35}_{-0.31})$	$244.5 \pm 7.5^{+8.2}_{-7.4}$
Belle [59]	$\tau^+\nu$ ($\mu^+\nu\bar{\nu}$)	$(5.86 \pm 0.37^{+0.34}_{-0.59})$	$255.4 \pm 8.0^{+7.6}_{-13.1}$
BES III [64]	$\tau^+\nu$ ($\pi^+\bar{\nu}$)	$(0.483 \pm 0.65 \pm 0.26)$	$231.9 \pm 15.7 \pm 6.5$
Our average	$\tau^+\nu$	(5.51 ± 0.20)	248.3 ± 6.1
Our average	$\mu^+\nu + \tau^+\nu$		245.7 ± 4.6

Babar and Belle use $e^+e^- \rightarrow DKn\pi D_s^*$ collisions at energies near the $\Upsilon(4S)$. CLEO and BES III do a similar analysis as was done for the D^+ above. Babar and Belle do a similar MM^2 calculation by using the reconstructed hadrons, the photon from the D_s^{*+} decay and a detected μ^+ . To get the normalization they do a MM^2 fit without the μ^+ and use the signal at the D_s^+ mass squared to determine the total D_s^+ yield.

When selecting the $\tau^+ \rightarrow \pi^+\bar{\nu}$ and $\tau^+ \rightarrow \rho^+\bar{\nu}$ decay modes, CLEO uses both the calculation of the missing-mass and the fact that there should be no extra energy in the event beyond that deposited by the measured tagged D_s^- and the τ^+ decay products. The $\tau^+ \rightarrow e^+\nu\bar{\nu}$ mode, however, uses only extra energy. Babar and Belle also use the extra energy to discriminate signal from background in their $\tau^+\nu$ measurements. BES III uses $\tau^+ \rightarrow \pi^+\bar{\nu}$ decays, where they calculate the MM^2 and discriminate against μ^+ from $D_s^+ \rightarrow \mu^+\nu$ decays.

When extracting $|V_{cs}|f_{D_s^+}$ via Eq. (84.1), we first apply the -1.8% universal electroweak correction [1] to all of the $\mu^+\nu$ and $\tau^+\nu$ branching fractions in Table 84.3; this is the same as for D^+ mesons. We also decrease the Babar and Belle $\mu^+\nu$ branching fractions by the 1% structure-dependent correction [14]. This correction was already included in CLEO and BES results for the $\mu^+\nu$ branching fractions in Table 84.3. We use the masses and lifetimes $m_{D_s^+} = 1.96834(7)$ GeV, $m_{\tau^+} = 1.7686(12)$ GeV, and $\tau_{D_s^+} = 0.504(4)$ ps [50]. The inferred values for $f_{D_s^+}|V_{cs}|$ are in good agreement for the $\mu^+\nu$ and $\tau^+\nu$ decay modes.

It is clear from the discussion of radiative corrections in this section that they are less well understood theoretically for D^+ and D_s^+ meson decays than for pions and kaons. We therefore assign a 2.8% systematic uncertainty to the purely leptonic decay rates, which is the full size of the applied radiative corrections. This translates to a 1.4% error on the products of the decay constant times CKM matrix element. Putting everything together, the main experimental pertaining

Table 84.4: Recent theoretical determinations of f_D , f_{D_s} , and their ratio in the isospin-symmetric limit. The upper panels show results from lattice-QCD simulations with $(2+1+1)$ and $(2+1)$ dynamical quark flavors, respectively. Statistical and systematic errors are quoted separately. The bottom panel shows estimates from QCD sum rules (QCD SR) and the light-front quark model (LFQM). These are not used to obtain our preferred decay-constant values.

Reference	Method	N_f	$f_D(\text{MeV})$	$f_{D_s}(\text{MeV})$	f_{D_s}/f_D
Fermilab/MILC 17 [34]	LQCD	2+1+1	212.1(0.3)(0.5)	249.9(0.3)(0.3)	1.1782(06)(15)*
ETM 14 [35]	LQCD	2+1+1	207.4(3.7)(0.9)	247.2(3.9)(1.4)	1.192(19)(11)
FLAG 19 average [18]	LQCD	2+1+1	212.0(0.7)	249.9(0.5)	1.1783(16)
RBC/UKQCD 18 [68] [†]	LQCD	2+1	–	–	1.1652(35) $\left(\begin{smallmatrix} +120 \\ -52 \end{smallmatrix}\right)$
RBC/UKQCD 17 [69]	LQCD	2+1	208.7(2.8) $\left(\begin{smallmatrix} +2.1 \\ -1.8 \end{smallmatrix}\right)$	246.4(1.3) $\left(\begin{smallmatrix} +1.3 \\ -1.9 \end{smallmatrix}\right)$	1.1667(77) $\left(\begin{smallmatrix} +57 \\ -43 \end{smallmatrix}\right)$
χ QCD 14 [70]	LQCD	2+1	–	254(2)(4)	–
HPQCD 12 [71]	LQCD	2+1	208.3(1.0)(3.3)	–	1.187(4)(12)
Fermilab/MILC 11 [72]	LQCD	2+1	218.9(9.2)(6.6)	260.1(8.9)(6.1)	1.188(14)(21)
HPQCD 10 [73]	LQCD	2+1	–	248.0(1.4)(2.1)	–
FLAG 19 average [18]	LQCD	2+1	209.0(2.4)	248.0(1.6)	1.174(7)
Wang 15 [74] [§]	QCD SR		208(10)	240(10)	1.15(6)
Gelhausen 13 [75]	QCD SR		201 $\left(\begin{smallmatrix} +12 \\ -13 \end{smallmatrix}\right)$	238 $\left(\begin{smallmatrix} +13 \\ -23 \end{smallmatrix}\right)$	1.15 $\left(\begin{smallmatrix} +0.04 \\ -0.05 \end{smallmatrix}\right)$
Narison 12 [76]	QCD SR		204(6)	246(6)	1.21(4)
Lucha 11 [77]	QCD SR		206.2(8.9)	245.3(16.3)	1.193(26)
Hwang 09 [78]	LFQM		–	264.5(17.5) [¶]	1.29(7)

* Ref. [34] provides values for f_D and f_{D_s} in the isospin-symmetric limit, but not for their ratio. Here we infer the central value from those of the individual decay constants, and take the statistical and systematic errors to be the same as for the physical ratio f_{D_s}/f_{D^+} .

[†] Preprint submitted to the arXiv and JHEP after the deadline for inclusion in the 2019 FLAG review.

[§] Obtained using m_c^{MS} ; results using m_c^{pole} are also given in the paper.

[¶] Obtained by combining PDG value $f_D = 205.8(8.9)$ MeV [79] with f_{D_s}/f_D from this work.

charmed meson leptonic decays are (see the bottom lines of Tables 84.2 and 84.3):

$$|V_{cd}|f_{D^+} = 46.2 \pm 1.0 \pm 0.6 \text{ MeV}, \quad (84.15)$$

$$|V_{cs}|f_{D_s^+} = 245.7 \pm 3.1 \pm 3.4 \text{ MeV}, \quad (84.16)$$

where the errors are from the measured branching fractions and the applied radiative corrections, respectively.

84.3.2 Theoretical decay-constant calculations

Table 84.4 presents recent theoretical calculations of charmed heavy-light meson decay constants and their ratio in the isospin-symmetric limit $m_u = m_d$. (As in Sec. 84.2.2, we denote the physical D^+ -meson decay constant by f_{D^+} , and use f_D for the isospin-symmetric value.) The upper two panels show results from lattice-QCD simulations with three ($N_f = 2+1$) or four flavors ($N_f = 2+1+1$) of dynamical quarks. Although there are fewer available results than for the pion and kaon sector, both f_D and f_{D_s} have been obtained using multiple sets of gauge-field configurations with different lattice fermion actions, providing independent confirmation. For comparison, the bottom panel of Table 84.4 shows QCD-model calculations of the D - and D_s -meson decay constants for which uncertainty estimates are provided. The lattice and non-lattice results agree, but numerical lattice-QCD simulations have now reached significantly greater precision than other approaches.

The lattice-QCD decay-constant results in Table 84.4 were all obtained using isospin-symmetric

gauge-field configurations. As discussed in Sec. 84.2.2, however, the leading strong-isospin breaking corrections to heavy-light pseudoscalar-meson decay constants can be accounted for by using the physical down (or up) quark in the D (or B) meson. Strong-isospin breaking corrections to heavy-strange meson decay constants are roughly an order-of-magnitude smaller because there are no light valence quarks involved. Recently, the Fermilab Lattice and MILC Collaborations used this approach to calculate directly the dominant strong-isospin breaking corrections to both f_D and f_B , finding [34]

$$f_{D^+} - f_D = 0.58(1)(7) \text{ MeV}, \quad f_{B^+} - f_B = -0.53(5)(7) \text{ MeV}. \quad (84.17)$$

These results agree with independent estimates of the strong-isospin-breaking corrections to heavy-light meson decay constants from Borelized sum rules [80]. Combined with the determinations of f_D and f_B from the same work, Eq. (84.17) implies that the corrections to the SU(3)-flavor breaking ratios are

$$\frac{f_{D_s}}{f_{D^+}} = \frac{f_{D_s}}{f_D} (1 - 0.0027(3)), \quad \frac{f_{B_s}}{f_{B^+}} = \frac{f_{B_s}}{f_B} (1 + 0.0028(5)). \quad (84.18)$$

These estimated strong-isospin-breaking corrections to f_D and f_{D_s}/f_D above are commensurate with the uncertainties on the (2+1+1)-flavor FLAG averages in Table 84.4. Consequently, it is important to account isospin-breaking effects before combining the theoretical decay constants with the corresponding experimental decay rates.

To obtain the charged D^+ -meson decay constant, we apply the correction in Eq. (84.17) to the (2+1+1)-flavor 2019 FLAG average for the D -meson decay constant in the isospin-symmetric limit. Similarly we use Eq. (84.18) to correct the (2+1+1)-flavor 2019 FLAG average for f_{D_s}/f_D . We take the four-flavor FLAG 2019 average for f_{D_s} directly. Our final preferred theoretical values for the charmed pseudoscalar-meson decay constants are

$$f_{D^+} = 212.6(7) \text{ MeV}, \quad f_{D_s} = 249.9(5) \text{ MeV}, \quad \frac{f_{D_s}}{f_{D^+}} = 1.175(2). \quad (84.19)$$

For all three quantities in Eq. (84.19), the uncertainties are roughly half the size of those in our previous review [26, 49].

84.4 Bottom mesons

84.4.1 *Experimental rate measurements*

The Belle and BaBar collaborations have found evidence for $B^- \rightarrow \tau^- \bar{\nu}$ decay in $e^+e^- \rightarrow B^- B^+$ collisions at the $\Upsilon(4S)$ energy. The analysis relies on reconstructing a hadronic or semi-leptonic B decay tag, finding a τ candidate in the remaining track and photon candidates, and examining the extra energy in the event which should be close to zero for a real τ^- decay to $e^- \nu \bar{\nu}$ or $\mu^- \nu \bar{\nu}$ opposite a B^+ tag. While the BaBar results have remained unchanged, Belle reanalyzed both samples of their data. The branching fraction using hadronic tags changed from $1.79^{+0.56+0.46}_{-0.49-0.51} \times 10^{-4}$ [81] to $0.72^{+0.27}_{-0.25} \pm 0.11 \times 10^{-4}$ [82], while the corresponding change using semileptonic tags was from $1.54^{+0.38+0.29}_{-0.37-0.31}$ to $1.25 \pm 0.28 \pm 0.27$. These changes demonstrate the difficulty of the analysis. The results are listed in Table 84.5.

Because there are large backgrounds under the signals for these measurements, as well as substantial systematic errors, the significances of the individual results are still below the 5σ discovery threshold. Belle quotes 4.6σ for their combined hadronic and semileptonic tags, while BaBar quotes 3.3σ and 2.3σ , for hadronic and semileptonic tags. Greater precision is necessary to determine if any effects beyond the Standard Model are present.

We do not correct the measured branching ratios in Table 84.5 for radiative corrections because the experimental uncertainties are so large. The radiative corrections are expected to be bigger,

Table 84.5: Experimental results for $\mathcal{B}(B^- \rightarrow \tau^- \bar{\nu})$ and $|V_{ub}|f_{B^+}$. To extract the values of $|V_{ub}|f_{B^+}$ via Eq. (84.1), we use the PDG 2018 value of the B^+ lifetime of 1.638 ± 0.004 ps, and the τ^+ and B^+ masses of 1.77686 and 5.27933 GeV, respectively.

Experiment	Tag	\mathcal{B} (units of 10^{-4})	$ V_{ub} f_{B^+}$ (MeV)
Belle [82]	Hadronic	$0.72_{-0.25}^{+0.27} \pm 0.11$	
Belle [83]	Semileptonic	$1.25 \pm 0.28 \pm 0.27$	
Belle [83]	Average	0.91 ± 0.22	0.72 ± 0.09
BaBar [84]	Hadronic	$1.83_{-0.49}^{+0.53} \pm 0.24$	
BaBar [85]	Semileptonic	$1.7 \pm 0.8 \pm 0.2$	
BaBar [84]	Average	1.79 ± 0.48	1.01 ± 0.14
Our average		1.06 ± 0.20	0.77 ± 0.07

however, for $B \rightarrow \mu\nu$ leptonic decays because the corrections are no longer helicity suppressed [6], and may be a significant fraction of the purely leptonic rate. More theoretical work is needed to understand radiative corrections to leptonic B decays in anticipation of future measurements with greater precision, and of new decay channels.

84.4.2 Theoretical decay-constant calculations

Table 84.6 presents recent theoretical calculations of bottom heavy-light meson decay constants and their ratio in the isospin-symmetric limit $m_u = m_d$. The upper two panels show results from lattice-QCD simulations with three ($N_f = 2 + 1$) or four flavors ($N_f = 2 + 1 + 1$) of dynamical quarks. For all decay constants, calculations using different gauge-field configurations, light-quark actions, and b -quark actions provide independent confirmation. For comparison, the bottom panel of Table 84.6 shows QCD-model calculations of the B^- and B_s^- -meson decay constants for which uncertainty estimates are provided. These are consistent with the lattice values, but with much larger uncertainties.

The lattice-QCD decay-constant results in Table 84.6 were all obtained using isospin-symmetric gauge-field configurations. Some calculations, however, account for the dominant effect of strong-isospin-breaking by using the correct value for the valence light-quark mass in the B meson (m_u for f_{B^+} and m_d for f_{B^0}). Early estimates of the strong-isospin-breaking correction obtained $f_{B^+} - f_B \sim 2$ MeV [88, 90], which would be significant given the present lattice-QCD uncertainties. It turns out, however, that these calculations inadvertently introduced a spurious sea-quark contribution, and therefore overestimated the size of the effect. A more recent calculation by the Fermilab/MILC Collaboration finds very little evidence for isospin violation ($f_{B^+} - f_B \sim 0.5$ MeV) [34], which is more than two times smaller than the total uncertainties on present lattice-QCD calculations. For this reason, we quote isospin averages in the current review.

Our preferred theoretical values for the bottom pseudoscalar-meson decay constants are

$$f_B = 190.0(1.3) \text{ MeV}, \quad f_{B_s} = 230.0(1.3) \text{ MeV}, \quad \frac{f_{B_s}}{f_B} = 1.209(5), \quad (84.20)$$

which are simply the $N_f = 2 + 1 + 1$ FLAG 2019 averages [18]. Because the uncertainties on the three-flavor results in Table 84.6 are substantially larger than those on the four-flavor results, including them in the average leaves the central values unchanged, and decreases the errors only slightly.

Table 84.6: Recent theoretical determinations of f_B , f_{B_s} , and their ratio in the isospin-symmetric limit. The upper panels show results from lattice-QCD simulations with $(2+1+1)$ and $(2+1)$ dynamical quark flavors, respectively. When available, statistical and systematic errors are quoted separately. The bottom panel shows estimates from the relativistic potential model (RPM), QCD sum rules, and the light-front quark model, which are not used to obtain our preferred decay-constant values.

Reference	Method	N_f	$f_B(\text{MeV})$	$f_{B_s}(\text{MeV})$	f_{B_s}/f_B
FNAL/MILC 17 [34]	LQCD	2+1+1	189.9(1.4)	230.7(1.2)	1.2180(49)
HPQCD 17 [86]*	LQCD	2+1+1	196(6)	236(7)	1.207(7)
ETM 16 [87]	LQCD	2+1+1	193(6)	229(5)	1.184(25)
HPQCD 13 [88]	LQCD	2+1+1	186(4)	224(5)	1.217(8)
FLAG 19 average [18]	LQCD	2+1+1	190.0(1.3)	230.3(1.3)	1.209(5)
Aoki 14 [89] [†]	LQCD	2+1	218.8(6.5)(30.8)	263.5(4.8)(36.7)	1.193(20)(44)
RBC/UKQCD 14 [90] [‡]	LQCD	2+1	195.6(6.4)(13.3)	235.4(5.2)(11.1)	1.223(14)(70)
HPQCD 12 [91]	LQCD	2+1	191(1)(8)	228(3)(10)	1.188(12)(13)
HPQCD 12 [91]	LQCD	2+1	189(3)(3)*	–	–
HPQCD 11 [92]	LQCD	2+1	–	225(3)(3)	–
Fermilab/MILC 11 [72]	LQCD	2+1	196.9(5.5)(7.0)	242.0(5.1)(8.0)	1.229(13)(23)
FLAG 19 average [18]	LQCD	2+1	192.0(4.3)	228.4(3.7)	1.201(16)
Sun 16 [93] [§]	RPM		219(15)	266(19)	1.21(9)
Wang 15 [74] [§]	QCD SR		194(15)	231(16)	1.19(10)
Baker 13 [94]	QCD SR		186(14)	222(12)	1.19(4)
Lucha 13 [95]	QCD SR		192.0(14.6)	228.0(19.8)	1.184(24)
Gelhausen 13 [75]	QCD SR		207 ⁽⁺¹⁷⁾ ₍₋₉₎	242 ⁽⁺¹⁷⁾ ₍₋₁₂₎	1.17 ⁽⁺³⁾ ₍₋₄₎
Narison 12 [76]	QCD SR		206(7)	234(5)	1.14(3)
Hwang 09 [78]	LFQM		–	270.0(42.8) [¶]	1.32(8)

* Re-analysis of data from HPQCD 13.

[†] Obtained with static b quarks (*i.e.* $m_b \rightarrow \infty$).

[‡] Ref. [90] does not provide results in the isospin-symmetric limit, so we show f_{B^+} and f_{B_s}/f_{B^+} for this work.

* Obtained by combining f_{B_s} from HPQCD 11 with f_{B_s}/f_B from this work. Approximate statistical (systematic) error obtained from quadrature sum of individual statistical (systematic) errors.

[§] Obtained using m_b^{MS} ; results using m_b^{pole} are also given in the paper.

[¶] Obtained by combining PDG value $f_B = 204(31)$ MeV [79] with f_{B_s}/f_B from this work.

84.5 Phenomenological implications

84.5.1 $|V_{ud}|$, $|V_{us}|$, and status of first-row unitarity

Using the average values for $f_{\pi^+}|V_{ud}|$, $f_{K^+}|V_{us}|$, and their ratio from Eqs. (84.10)–(84.12) and for f_{π^+} , f_{K^+} , and their ratio from Eq. (84.14), we obtain the following determinations of the CKM matrix elements $|V_{ud}|$, $|V_{us}|$, and their ratio from leptonic decays within the standard model:

$$|V_{ud}| = 0.9764(2)(90)(10), \quad |V_{us}| = 0.2254(3)(4)(3), \quad \frac{|V_{us}|}{|V_{ud}|} = 0.2313(2)4(2), \quad (84.21)$$

where the errors are from the experimental branching fraction(s), the pseudoscalar decay constant(s), and radiative corrections, respectively. These results enable a precise test of the unitarity of the first row of the CKM matrix from leptonic decays alone (the contribution from $|V_{ub}|$ is

negligible). Using the values of $|V_{ud}|$ and $|V_{us}|$ from Eq. (84.21), we find

$$|V_{ud}|^2 + |V_{us}|^2 + |V_{ub}|^2 - 1 = 0.004(18), \quad (84.22)$$

which is consistent with three-generation unitarity at the few-percent level.

The determinations of $|V_{ud}|$ and $|V_{us}|$ from leptonic decays in Eq. (84.21) can be compared to those obtained from other processes. The result above for $|V_{ud}|$ agrees with the determination from superallowed β -decay, $|V_{ud}| = 0.97420(21)$ [96], but has an error about forty times larger that is primarily due to the uncertainty in the theoretical determination of f_{π^+} . The CKM element $|V_{us}|$ can be determined from semileptonic $K^+ \rightarrow \pi^0 \ell^+ \nu$ decay. Here experimental measurements provide a value for the product $f_+^{K\pi}(0)|V_{us}|$, where $f_+^{K\pi}(0)$ is the form-factor at zero four-momentum transfer between the initial state kaon and the final state pion. Taking the most recent experimental determination of $|V_{us}|f_+^{K\pi}(0) = 0.2165(4)$ from Moulson [28]⁶ and the 2019 (2+1+1)-flavor FLAG average for $f_+(0)^{K\pi} = 0.9706(27)$ [18] based on the calculations of ETM [100] and Fermilab/MILC [101] gives $|V_{us}| = 0.2231(6)_{\text{LQCD}(4)_{\text{exp}}}$ from $K_{\ell 3}$ decay. The determinations of $|V_{us}|$ from leptonic and semileptonic kaon decays are both quite precise (with the error from leptonic decay being about 25% smaller), but the central values differ by 2.5σ . (This difference would be reduced to 1.8σ , but not eliminated, using the (2+1)-flavor FLAG average for $f_+(0)^{K\pi} = 0.9677(27)$ instead.) Finally, the combination of the ratio $|V_{us}|/|V_{ud}|$ from leptonic decays [Eq. (84.21)] with $|V_{ud}|$ from β decay implies an alternative determination of $|V_{us}| = 0.2254(5)$ which agrees with the value from leptonic kaon decay, but disagrees with the $K_{\ell 3}$ -decay result at the 1.8σ level.

Given the roughly 2σ tension between $|V_{us}|$ from leptonic and semileptonic kaon decays, it is important to scrutinize the uncertainties on the theoretical and experimental inputs to $|V_{us}|$ and other elements of the first row of the CKM matrix. Recently, Seng *et al.* introduced a new approach for calculating radiative corrections to neutron and nuclear beta decays using dispersion relations [102–105]. These calculations imply a lower value of $|V_{ud}| = 0.97395(23)$ than the Hardy and Towner analysis [106] by almost 1σ . An independent calculation of the radiative corrections by Czarnecki and Marciano using QCD sum rules yields similar results [107]. Using this value of $|V_{ud}|$ with the determination of $|V_{us}|$ from leptonic kaon decays in Eq. (84.21), we obtain $|V_{ud}|^2 + |V_{us}|^2 + |V_{ub}|^2 - 1 = -0.0006(5)$, again (roughly) consistent with first-row unitarity.

Last, we combine the experimental measurement of $f_{\pi^+}|V_{ud}|$ in Eq. (84.10) with $|V_{ud}|$ from superallowed β -decay [96] to infer an “experimental” value for the pion decay constant:

$$f_{\pi^-}^{\text{“exp”}} = 130.50(2)(3)(13) \text{ MeV}, \quad (84.23)$$

where the uncertainties are from the errors on Γ , $|V_{ud}|$, and higher-order corrections, respectively. Many recent (2+1+1)-flavor lattice-QCD calculations use this quantity to set the overall physical scale in their simulations, *e.g.*, Refs. [7, 34–36]. Conversely, comparing $f_{\pi^-}^{\text{“exp”}}$ with the 2019 FLAG (2+1)-flavor average $f_{\pi^+} = 130.2(8)$ MeV, which only includes lattice-QCD results that employ observables to set the scale [37–42], provides a test of lattice-QCD methods. The values are in good agreement within present uncertainties. We do not quote an “experimental” value for the kaon decay constant because the value of $|V_{us}|$ is less clear given the $\sim 2\sigma$ tension between the values of $|V_{us}|$ obtained from leptonic and semileptonic kaon decays.

84.5.2 $|V_{cd}|$, $|V_{cs}|$, and status of second-row unitarity

Using the average values for $|V_{cd}|f_{D^+}$ and $|V_{cs}|f_{D_s^+}$ from Eqs. (84.15) and (84.16), and for f_{D^+} and $f_{D_s^+}$ from Eq. (84.19), we obtain the following determinations of the CKM matrix elements

⁶This is an update of the 2010 Flavianet review [29] that includes new measurements of the K_S lifetime [97, 98], $\text{Re}(\epsilon'/\epsilon)$ [98], and $\mathcal{B}(K^\pm \rightarrow \pi^\pm \pi^+ \pi^-)$ [99]. The latter measurement is the primary source of the reduced error on $\mathcal{B}(K_{\ell 3})$, via the constraint that the sum of all branching ratios must equal unity.

$|V_{cd}|$ and $|V_{cs}|$ from leptonic decays within the standard model:

$$|V_{cd}| = 0.217(5)(3)(1) \quad \text{and} \quad |V_{cs}| = 0.983(13)(14)(2), \quad (84.24)$$

where the errors are from the measured branching fractions, radiative corrections, and decay constants, respectively. These results enable a test of the unitarity of the second row of the CKM matrix. We obtain

$$|V_{cd}|^2 + |V_{cs}|^2 + |V_{cb}|^2 - 1 = 0.016(37), \quad (84.25)$$

in agreement with three-generation unitarity.

The uncertainty on $|V_{cd}|$ in Eq. (84.24) is limited by the measurement error on the $D^+ \rightarrow \mu^+ \nu$ decay rate. For $|V_{cs}|$, however, the experimental and radiative-correction errors are commensurate. It is worth noting that the value of $|V_{cs}|$ from leptonic D_s decays has decreased substantially from the value of 1.007(17) in the previous version of this review [26, 49], and is now below unity as expected in the three-generation CKM framework. This change is due to our new, more consistent treatment of the radiative corrections, which lower the purely leptonic decay rates for the $\mu^+ \nu$ and $\tau^+ \nu$ channels by 2.8% and 1%, respectively. We emphasize, however, that we have taken a generous 100% uncertainty on these estimates, and that more theoretical work is needed to really pin down the sizes of the radiative corrections to $D_{(s)}$ -meson leptonic decays.

The CKM matrix elements $|V_{cd}|$ and $|V_{cs}|$ can also be obtained from semileptonic $D^+ \rightarrow \pi^0 \ell^+ \nu$ and $D_s^+ \rightarrow K^0 \ell^+ \nu$ decays, respectively. Here experimental measurements determine the product of the form factor times the CKM element, and theory provides the value for the form factor at zero four-momentum transfer between the initial $D_{(s)}$ meson and the final pion or kaon. The latest experimental averages from the Heavy Flavor Averaging Group (HFLAV) are $f_+^{D\pi}(0)|V_{cd}| = 0.1426(19)$ and $f_+^{D_s K}(0)|V_{cs}| = 0.7226(34)$ [108]. There are not enough published lattice-QCD calculations of the zero-momentum $D_{(s)}$ -meson semileptonic form factors with $N_f \geq 3$ to permit an average by the FLAG Collaboration. Taking the most precise three-flavor form-factor results $f_+^{D\pi}(0) = 0.666(29)$ and $f_+^{D_s K}(0) = 0.747(19)$ from the HPQCD Collaboration [109, 110] gives for the CKM matrix elements $|V_{cd}| = 0.2141(97)$ and $|V_{cs}| = 0.967(25)$, in agreement with those from leptonic decays in Eq. (84.24). A newer, four-flavor calculation of the form factors by the ETM Collaboration, however, yields a smaller value of $f_+^{D\pi}(0) = 0.612(35)$ by 1.2σ and a larger $f_+^{D_s K}(0) = 0.765(31)$ by 0.5σ . These imply $|V_{cd}| = 0.233(14)$ and $|V_{cs}| = 0.945(39)$, which are about 1σ above and below the values from leptonic decays in Eq. (84.24), respectively. Independent lattice-QCD calculations of the $D^+ \rightarrow \pi^0 \ell^+ \nu$ and $D_s^+ \rightarrow K^0 \ell^+ \nu$ form factors now in progress [111, 112] may help clarify the picture.

We can combine the experimental measurements of $f_{D^+}|V_{cd}|$ and $f_{D_s^+}|V_{cs}|$ from Tables 84.2 and 84.3 with $|V_{cd}| = 0.22438(44)$ and $|V_{cs}| = 0.97359(10)$ from the PDG 2018 global unitarity-triangle analysis [50] to infer “experimental” values for the decay constants within the standard model. We take the CKM elements from the global fit because they are based on many input quantities, thereby reducing the sensitivity to any one outlying measurement or calculation. We obtain for the decay constants

$$f_{D^+}^{\text{“exp”}} = 205.8(4.5)(0.4)(2.7) \text{ MeV}, \quad f_{D_s^+}^{\text{“exp”}} = 252.4(3.2)(0.03)(3.5) \text{ MeV}, \quad (84.26)$$

$$\left(\frac{f_{D_s^+}}{f_{D^+}} \right)^{\text{“exp”}} = 1.226(31)(2)(3). \quad (84.27)$$

where the uncertainties are from the errors on $\Gamma^{(0)}$, CKM matrix elements, and radiative corrections, respectively. For the decay-constant ratio, we expect most of the radiative corrections

to cancel, and therefore multiply the 1.4% error from Sec. 84.3.1 by the SU(3)-breaking factor $(m_s - m_d)/\Lambda_{\text{QCD}} \sim 1/5$. The “experimental” values f_{D^+} ($f_{D_s^+}/f_{D^+}$) are about 1.3σ lower (1.6σ higher) than the (2+1+1)-flavor lattice-QCD averages in Eq. (84.19). The CKM matrix element $|V_{cd}|$ is, however, proportional to $|V_{us}|$ within the Wolfenstein parameterization [113, 114]. Thus, resolving the inconsistencies between determinations of $|V_{us}|$ from leptonic and semileptonic decays discussed in Sec. 84.5.1 may also reduce the mild tensions observed here.

Last, we can test lepton-flavor universality in charm meson decays by checking the following relationship derived from Eq. (84.1):

$$\frac{\Gamma(D_s^+ \rightarrow \tau^+\nu)}{\Gamma(D_s^+ \rightarrow \mu^+\nu)} = \frac{m_\tau^2 \left(1 - m_\tau^2/M_{D_s}^2\right)^2}{m_\mu^2 \left(1 - m_\mu^2/M_{D_s}^2\right)^2} = 9.75, \quad (84.28)$$

where the uncertainties from the masses are negligible to the number of digits quoted. The measured ratio of $\tau^+\nu$ to $\mu^+\nu$ rates is 9.98 ± 0.46 , consistent with the standard-model expectation.

84.5.3 $|V_{ub}|$ and other applications

Using the average value for $|V_{ub}|f_{B^+}$ from Table 84.5, and for f_{B^+} from Eq. (84.20), we obtain the following determination of the CKM matrix element $|V_{ub}|$ from leptonic decays within the standard model:

$$|V_{ub}| = 4.05(37)(3) \times 10^{-3}, \quad (84.29)$$

where the errors are from experiment and theory, respectively. One should bear in mind when interpreting Eq. (84.29) that none of the experimental measurements that enter the average for $|V_{ub}|f_{B^+}$ have individually reached the 5σ discovery level (see Sec. 84.4.1). Further, decays involving the third generation of quarks and leptons may be particularly sensitive to new physics associated with electroweak symmetry breaking due to their larger masses [10, 12], so Eq. (84.29) is more likely to be influenced by new physics than the determinations of the elements of the first and second rows of the CKM matrix in the previous sections.

The CKM element $|V_{ub}|$ can also be obtained from semileptonic B -meson decays. For more than a decade, there has remained a persistent $2\text{--}3\sigma$ tension between the determinations of $|V_{ub}|$ from exclusive $B \rightarrow \pi\ell\nu$ decay and from inclusive $B \rightarrow X_u\ell\nu$ decay, where X_u denotes all hadrons which contain a constituent up quark [21, 108, 115–118]. The currently most precise determination of $|V_{ub}|^{\text{excl}} = 3.73(14) \times 10^{-3}$ is obtained from a joint z -fit by FLAG [18] of the vector and scalar form factors $f_+^{B\pi}(q^2)$ and $f_0^{B\pi}(q^2)$ calculated in (2+1)-flavor lattice QCD [119–121] and experimental measurements of the differential decay rate from BaBar [122, 123] and Belle [124, 125]. On the other hand, the PDG 2018 inclusive determination obtained using the theoretical frameworks in Refs. [126–128] is $|V_{ub}|^{\text{incl}} = 4.49(28) \times 10^{-3}$ [50, 129]. The value of $|V_{ub}|$ from leptonic $B \rightarrow \tau\nu$ decay in Eq. (84.29) splits the difference between the inclusive and exclusive determinations, and is compatible (within large uncertainties) with both.

Given the large uncertainties on the experimental measurements of $\mathcal{B}(B^- \rightarrow \tau^-\bar{\nu})$, and the more than 2σ disagreement between $|V_{ub}|$ obtained from inclusive and exclusive semileptonic B decays, we do not present an “experimental” value of the decay constant f_{B^+} .

Acknowledgements

We thank V. Cirigliano, C. Davies, A. El Khadra, A. Khodjamirian, A. Kronfeld, J. Laiho, W. Marciano, M. Moulson, S. Narison, S. Sharpe, and Z.-G. Wang for useful discussions on this and previous versions of the review. We thank M. Della Morte and S. Simula for valuable feedback on the manuscript, and for providing information on the 2019 FLAG lattice averages. We gratefully acknowledge support of the U. S. National Science Foundation and the U. S. Department of Energy

through Grant No. DE-FG02-13ER41598. The work of J. L. R. was performed in part at the Aspen Center for Physics, which is supported by National Science Foundation grant PHY-1066293. Fermilab is operated by the Fermi Research Alliance, LLC, under Contract No. DE-AC02-07CH11359 with the U.S. Department of Energy, Office of Science, Office of High Energy Physics.

References

- [1] A. Sirlin, Nucl. Phys. **B196**, 83 (1982).
- [2] T. Kinoshita, Phys. Rev. Lett. **2**, 477 (1959).
- [3] M. Knecht *et al.*, Eur. Phys. J. **C12**, 469 (2000), [hep-ph/9909284].
- [4] G. Burdman, J. T. Goldman and D. Wyler, Phys. Rev. **D51**, 111 (1995), [hep-ph/9405425].
- [5] V. Cirigliano and I. Rosell, JHEP **10**, 005 (2007), [arXiv:0707.4464].
- [6] D. Becirevic, B. Haas and E. Kou, Phys. Lett. **B681**, 257 (2009), [arXiv:0907.1845].
- [7] A. Bazavov *et al.* (Fermilab Lattice and MILC), Phys. Rev. **D90**, 074509 (2014), [arXiv:1407.3772].
- [8] M. Di Carlo *et al.*, Phys. Rev. **D100**, 034514 (2019), [arXiv:1904.08731].
- [9] E. Barberio and Z. Was, Comput. Phys. Commun. **79**, 291 (1994).
- [10] W.-S. Hou, Phys. Rev. **D48**, 2342 (1993).
- [11] A. G. Akeroyd and S. Recksiegel, Phys. Lett. **B554**, 38 (2003), [hep-ph/0210376].
- [12] A. G. Akeroyd and S. Recksiegel, J. Phys. **G29**, 2311 (2003), [hep-ph/0306037].
- [13] A. G. Akeroyd, Prog. Theor. Phys. **111**, 295 (2004), [hep-ph/0308260].
- [14] B. A. Dobrescu and A. S. Kronfeld, Phys. Rev. Lett. **100**, 241802 (2008), [arXiv:0803.0512].
- [15] J. L. Hewett, in “Heavy flavor physics. Proceedings, LISHEP 95, LAFEX International School on High-Energy Physics, session C, cbt Workshop, Rio de Janeiro, Brazil, February 21-23, 1995,” 171–187 (1995), [hep-ph/9505246], URL <http://www-public.slac.stanford.edu/sciDoc/docMeta.aspx?slacPubNumber=SLAC-PUB-6821>.
- [16] A. Crivellin, Phys. Rev. **D81**, 031301 (2010), [arXiv:0907.2461].
- [17] F. U. Bernlochner, Z. Ligeti and S. Turczyk, Phys. Rev. **D90**, 094003 (2014), [arXiv:1408.2516].
- [18] S. Aoki *et al.* (Flavour Lattice Averaging Group) (2019), [arXiv:1902.08191].
- [19] W. J. Marciano, Phys. Rev. Lett. **93**, 231803 (2004), [hep-ph/0402299].
- [20] V. Cirigliano *et al.*, Rev. Mod. Phys. **84**, 399 (2012), [arXiv:1107.6001].
- [21] K. A. Olive *et al.* (Particle Data Group), Chin. Phys. **C38**, 090001 (2014).
- [22] B. Ananthanarayan and B. Moussallam, JHEP **06**, 047 (2004), [hep-ph/0405206].
- [23] S. Descotes-Genon and B. Moussallam, Eur. Phys. J. **C42**, 403 (2005), [hep-ph/0505077].
- [24] W. J. Marciano and A. Sirlin, Phys. Rev. Lett. **71**, 3629 (1993).
- [25] V. Cirigliano and H. Neufeld, Phys. Lett. **B700**, 7 (2011), [arXiv:1102.0563].
- [26] J. L. Rosner, S. Stone and R. S. Van de Water (2015), review prepared for PDG 2015 edition, [arXiv:1509.02220].
- [27] J. Gasser, A. Rusetsky and I. Scimemi, Eur. Phys. J. **C32**, 97 (2003), [hep-ph/0305260].
- [28] M. Moulson, in “8th International Workshop on the CKM Unitarity Triangle (CKM2014) Vienna, Austria, September 8-12, 2014,” (2014), [arXiv:1411.5252].
- [29] M. Antonelli *et al.* (FlaviaNet Working Group on Kaon Decays), Eur. Phys. J. **C69**, 399 (2010), [arXiv:1005.2323].

- [30] S. Hashimoto, J. Laiho and S. R. Sharpe, “Lattice Quantum Chromodynamics,” <http://pdg.lbl.gov/2019/reviews/rpp2018-rev-lattice-qcd.pdf> (2017), review prepared for PDG 2018 edition.
- [31] S. Aoki *et al.* (Flavour Lattice Averaging Group), *Eur. Phys. J.* **C74**, 2890 (2014), [arXiv:1310.8555].
- [32] S. Aoki *et al.*, *Eur. Phys. J.* **C77**, 2, 112 (2017), [arXiv:1607.00299].
- [33] A. S. Kronfeld, *Ann. Rev. Nucl. Part. Sci.* **62**, 265 (2012), [arXiv:1203.1204].
- [34] A. Bazavov *et al.*, *Phys. Rev.* **D98**, 7, 074512 (2018), [arXiv:1712.09262].
- [35] N. Carrasco *et al.* (ETM), *Phys. Rev.* **D91**, 054507 (2015), [arXiv:1411.7908].
- [36] R. Dowdall *et al.* (HPQCD), *Phys. Rev.* **D88**, 074504 (2013), [arXiv:1303.1670].
- [37] V. G. Bornyakov *et al.* (QCDSF-UKQCD), *Phys. Lett.* **B767**, 366 (2017), [arXiv:1612.04798].
- [38] S. Durr *et al.*, *Phys. Rev.* **D95**, 5, 054513 (2017), [arXiv:1601.05998].
- [39] T. Blum *et al.* (RBC, UKQCD), *Phys. Rev.* **D93**, 074505 (2016), [arXiv:1411.7017].
- [40] A. Bazavov *et al.* (MILC), *PoS LATTICE2010*, 074 (2010), [arXiv:1012.0868].
- [41] S. Durr *et al.* (BMW), *Phys. Rev.* **D81**, 054507 (2010), [arXiv:1001.4692].
- [42] E. Follana *et al.* (HPQCD, UKQCD), *Phys. Rev. Lett.* **100**, 062002 (2008), [arXiv:0706.1726].
- [43] A. V. Manohar, C. T. Sachrajda and R. M. Barnett, “Quark Masses,” <http://pdg.lbl.gov/2019/reviews/rpp2018-rev-quark-masses.pdf> (2018), review prepared for PDG 2018 update.
- [44] G. M. de Divitiis *et al.*, *JHEP* **04**, 124 (2012), [arXiv:1110.6294].
- [45] J. Gasser and H. Leutwyler, *Nucl. Phys.* **B250**, 465 (1985).
- [46] G. M. de Divitiis *et al.* (RM123), *Phys. Rev.* **D87**, 11, 114505 (2013), [arXiv:1303.4896].
- [47] M. Nobes (2005), [hep-lat/0501009].
- [48] A. Bazavov *et al.* (Fermilab Lattice, MILC), *Phys. Rev.* **D93**, 11, 113016 (2016), [arXiv:1602.03560].
- [49] C. Patrignani *et al.* (Particle Data Group), *Chin. Phys.* **C40**, 10, 100001 (2016).
- [50] M. Tanabashi *et al.* (Particle Data Group), *Phys. Rev.* **D98**, 3, 030001 (2018).
- [51] M. Artuso *et al.* (CLEO), *Phys. Rev. Lett.* **95**, 251801 (2005), [hep-ex/0508057].
- [52] B. I. Eisenstein *et al.* (CLEO), *Phys. Rev.* **D78**, 052003 (2008), [arXiv:0806.2112].
- [53] M. Ablikim *et al.* (BESIII), *Phys. Rev.* **D89**, 051104 (2014), [arXiv:1312.0374].
- [54] M. Artuso *et al.* (CLEO), *Phys. Rev. Lett.* **99**, 071802 (2007), [arXiv:0704.0629].
- [55] J. P. Alexander *et al.* (CLEO), *Phys. Rev.* **D79**, 052001 (2009), [arXiv:0901.1216].
- [56] M. Ablikim *et al.* (BESIII) (2019), [arXiv:1908.08877].
- [57] J. P. Lees *et al.* (BaBar) (2010), [arXiv:1003.3063].
- [58] P. del Amo Sanchez *et al.* (BaBar), *Phys. Rev.* **D82**, 091103 (2010), [Erratum: *Phys. Rev.* **D91**, no.1, 019901 (2015)], [arXiv:1008.4080].
- [59] A. Zupanc *et al.* (Belle), *JHEP* **1309**, 139 (2013), [arXiv:1307.6240].
- [60] M. Ablikim *et al.* (BESIII), *Phys. Rev. Lett.* **122**, 071802 (2019), [arXiv:1811.10890].
- [61] P. Naik *et al.* (CLEO), *Phys. Rev.* **D80**, 112004 (2009), [arXiv:0910.3602].
- [62] K. M. Ecklund *et al.* (CLEO), *Phys. Rev. Lett.* **100**, 161801 (2008), [arXiv:0712.1175].

- [63] P. U. E. Onyisi *et al.* (CLEO), Phys. Rev. **D79**, 052002 (2009), [arXiv:0901.1147].
- [64] M. Ablikim *et al.* (BESIII), Phys. Rev. **D94**, 072004 (2016), [arXiv:1608.06732].
- [65] T. K. Pedlar *et al.* (CLEO), Phys. Rev. **D76**, 072002 (2007), [arXiv:0704.0437].
- [66] J. P. Alexander *et al.* (CLEO), Phys. Rev. Lett. **100**, 161804 (2008), [arXiv:0801.0680].
- [67] B. Aubert *et al.* (BaBar), Phys. Rev. Lett. **98**, 141801 (2007), [hep-ex/0607094].
- [68] P. A. Boyle *et al.* (RBC/UKQCD) (2018), [arXiv:1812.08791].
- [69] P. A. Boyle *et al.*, JHEP **12**, 008 (2017), [arXiv:1701.02644].
- [70] Y.-B. Yang *et al.* (χ QCD), Phys. Rev. **D92**, 034517 (2015), [arXiv:1410.3343].
- [71] H. Na *et al.* (HPQCD), Phys. Rev. **D86**, 054510 (2012), [arXiv:1206.4936].
- [72] A. Bazavov *et al.* (Fermilab Lattice and MILC), Phys. Rev. **D85**, 114506 (2012), [arXiv:1112.3051].
- [73] C. T. H. Davies *et al.* (HPQCD), Phys. Rev. **D82**, 114504 (2010), [arXiv:1008.4018].
- [74] Z.-G. Wang, Eur. Phys. J. **C75**, 427 (2015), [arXiv:1506.01993].
- [75] P. Gelhausen *et al.*, Phys.Rev. **D88**, 014015 (2013), [arXiv:1305.5432].
- [76] S. Narison, Phys. Lett. **B718**, 1321 (2013), [arXiv:1209.2023].
- [77] W. Lucha, D. Melikhov and S. Simula, Phys. Lett. **B701**, 82 (2011), [arXiv:1101.5986].
- [78] C.-W. Hwang, Phys. Rev. **D81**, 054022 (2010), [arXiv:0910.0145].
- [79] C. Amsler *et al.* (Particle Data Group), Phys. Lett. **B667**, 1 (2008), and 2009 partial update for the 2010 edition.
- [80] W. Lucha, D. Melikhov and S. Simula, Eur. Phys. J. **C78**, 2, 168 (2018), [Erratum: Eur. Phys. J.C78,no.11,936(2018)], [arXiv:1702.07537].
- [81] K. Ikado *et al.* (Belle), Phys. Rev. Lett. **97**, 251802 (2006), [hep-ex/0604018].
- [82] I. Adachi *et al.* (Belle), Phys. Rev. Lett. **110**, 131801 (2013), [arXiv:1208.4678].
- [83] B. Kronenbitter *et al.* (Belle), Phys. Rev. **D92**, 051102 (2015), [arXiv:1503.05613].
- [84] J. P. Lees *et al.* (BaBar), Phys. Rev. **D88**, 031102 (2013), [arXiv:1207.0698].
- [85] B. Aubert *et al.* (BaBar), Phys. Rev. **D81**, 051101 (2010), [arXiv:0912.2453].
- [86] C. Hughes, C. T. H. Davies and C. J. Monahan, Phys. Rev. **D97**, 5, 054509 (2018), [arXiv:1711.09981].
- [87] A. Bussone *et al.* (ETM), Phys. Rev. **D93**, 11, 114505 (2016), [arXiv:1603.04306].
- [88] R. Dowdall *et al.* (HPQCD), Phys. Rev. Lett. **110**, 222003 (2013), [arXiv:1302.2644].
- [89] Y. Aoki *et al.*, Phys. Rev. **D91**, 114505 (2015), [arXiv:1406.6192].
- [90] N. H. Christ *et al.* (RBC/UKQCD), Phys. Rev. **D91**, 054502 (2015), [arXiv:1404.4670].
- [91] H. Na *et al.* (HPQCD), Phys. Rev. **D86**, 034506 (2012), [arXiv:1202.4914].
- [92] C. McNeile *et al.* (HPQCD), Phys. Rev. **D85**, 031503 (2012), [arXiv:1110.4510].
- [93] H.-K. Sun and M.-Z. Yang, Phys. Rev. **D95**, 11, 113001 (2017), [arXiv:1609.08958].
- [94] M. J. Baker *et al.*, JHEP **07**, 032 (2014), [arXiv:1310.0941].
- [95] W. Lucha, D. Melikhov and S. Simula, Phys.Rev. **D88**, 056011 (2013), [arXiv:1305.7099].
- [96] J. Hardy and I. S. Towner, PoS **CKM2016**, 028 (2016).
- [97] F. Ambrosino *et al.* (KLOE), Eur. Phys. J. **C71**, 1604 (2011), [arXiv:1011.2668].
- [98] E. Abouzaid *et al.* (KTeV), Phys. Rev. **D83**, 092001 (2011), [arXiv:1011.0127].

- [99] D. Babusci *et al.* (KLOE KLOE-2), Phys. Lett. **B738**, 128 (2014), [arXiv:1407.2028].
- [100] N. Carrasco *et al.*, Phys. Rev. **D93**, 11, 114512 (2016), [arXiv:1602.04113].
- [101] A. Bazavov *et al.* (Fermilab Lattice and MILC), Phys. Rev. Lett. **112**, 112001 (2014), [arXiv:1312.1228].
- [102] C.-Y. Seng *et al.*, Phys. Rev. Lett. **121**, 241804 (2018), [arXiv:1807.10197].
- [103] C. Y. Seng, M. Gorchtein and M. J. Ramsey-Musolf, Phys. Rev. **D100**, 013001 (2019), [arXiv:1812.03352].
- [104] M. Gorchtein, Phys. Rev. Lett. **123**, 042503 (2019), [arXiv:1812.04229].
- [105] C.-Y. Seng and U.-G. Meißner, Phys. Rev. Lett. **122**, 211802 (2019), [arXiv:1903.07969].
- [106] J. C. Hardy and I. S. Towner, Phys. Rev. **C91**, 025501 (2015), [arXiv:1411.5987].
- [107] A. Czarnecki, W. J. Marciano and A. Sirlin (2019), [arXiv:1907.06737].
- [108] Y. Amhis *et al.* (HFLAV), Eur. Phys. J. **C77**, 12, 895 (2017), [arXiv:1612.07233].
- [109] H. Na *et al.* (HPQCD), Phys. Rev. **D82**, 114506 (2010), [arXiv:1008.4562].
- [110] H. Na *et al.* (HPQCD), Phys. Rev. **D84**, 114505 (2011), [arXiv:1109.1501].
- [111] B. Chakraborty *et al.*, EPJ Web Conf. **175**, 13027 (2018), [arXiv:1710.07334].
- [112] R. Li *et al.* (Fermilab Lattice, MILC), PoS **LATTICE2018**, 269 (2019), [arXiv:1901.08989].
- [113] L. Wolfenstein, Phys. Rev. Lett. **51**, 1945 (1983).
- [114] J. Charles *et al.* (CKMfitter Group), Eur. Phys. J. **C41**, 1 (2005), updated results and plots available at: <http://ckmfitter.in2p3.fr>, [hep-ph/0406184].
- [115] M. Antonelli *et al.*, Phys. Rept. **494**, 197 (2010), [arXiv:0907.5386].
- [116] J. N. Butler *et al.* (Quark Flavor Physics Working Group), in “Community Summer Study 2013: Snowmass on the Mississippi (CSS2013) Minneapolis, MN, USA, July 29-August 6, 2013,” (2013), [arXiv:1311.1076], URL <http://www.slac.stanford.edu/econf/C1307292/docs/IntensityFrontier/QuarkF1-15.pdf>.
- [117] Y. Amhis *et al.* (Heavy Flavor Averaging Group) (2014), [arXiv:1412.7515].
- [118] A. J. Bevan *et al.* (Belle, BaBar), Eur. Phys. J. **C74**, 3026 (2014), [arXiv:1406.6311].
- [119] E. Dalgic *et al.*, Phys. Rev. **D73**, 074502 (2006), [Erratum: Phys. Rev.D75,119906(2007)], [hep-lat/0601021].
- [120] J. M. Flynn *et al.* (RBC/UKQCD), Phys. Rev. **D91**, 074510 (2015), [arXiv:1501.05373].
- [121] J. A. Bailey *et al.* (Fermilab Lattice, MILC), Phys. Rev. **D92**, 014024 (2015), [arXiv:1503.07839].
- [122] P. del Amo Sanchez *et al.* (BaBar), Phys. Rev. **D83**, 032007 (2011), [arXiv:1005.3288].
- [123] J. P. Lees *et al.* (BaBar), Phys. Rev. **D86**, 092004 (2012), [arXiv:1208.1253].
- [124] H. Ha *et al.* (Belle), Phys. Rev. **D83**, 071101 (2011), [arXiv:1012.0090].
- [125] A. Sibidanov *et al.* (Belle), Phys.Rev. **D88**, 032005 (2013), [arXiv:1306.2781].
- [126] S. W. Bosch *et al.*, Phys. Rev. Lett. **93**, 221801 (2004), [hep-ph/0403223].
- [127] J. R. Andersen and E. Gardi, JHEP **01**, 097 (2006), [hep-ph/0509360].
- [128] P. Gambino *et al.*, JHEP **10**, 058 (2007), [arXiv:0707.2493].
- [129] R. Kowalewski and T. Mannel, “Semileptonic b -Hadron Decays, Determination of V_{cb} , V_{ub} ,” <http://pdg.lbl.gov/2019/reviews/rpp2018-rev-vcb-vub.pdf> (2017), review prepared for PDG 2018 update.